ISOPHOT*APERTURE SEQUENCES ON POINT- AND EXTENDED SOURCES

T.G. Müller
ISO Data Centre, ESA Astrophysics Division, Villafranca del Castillo, P.O. Box 50727, 28080 Madrid, Spain

ABSTRACT

ISOPHOT Multi-aperture measurements PHT04 have been used to search for extended emission around point sources (circumstellar disks, envelopes), extended structures (galaxies, diffuse interstellar medium, comets), companions, brightness distributions (galaxies, comet coma, comet tails) and nucleus/disk separation in galaxies.

Here the results from the PHT04 calibration observations on point sources and the applications of the results to scientific programmes are presented. In parallel to the measurements a Point Spread Function (PSF) model has been developed to simulate aperture sequences on point and different types of extended sources, including different levels of background contribution.

The combination of model parameters with the calibration data allows now to analyse the scientific PHT04 programmes. First results with structures around point sources are presented. A comparison of a PHT04 aperture sequence with ISOCAM observations on HD 97300 (Siebenmorgen et al., 1998) confirms the reliability of this mode by taking into account the findings from Paper I (Müller, 1999).

Key words: ISO; Infrared Astronomy; Multi-Aperture Photometry; Extended Sources; HD 97300.

1. INTRODUCTION

The detectors P1, P2 and P3 of the ISOPHOT instrument (Lemke et al., 1996) on board ISO (Kessler et al., 1996) have been used in combination with a set of different apertures to search for extended sources and to determine the size and profile of the extended structures. The filters of the P-detectors cover the wavelength range from $3.29\mu m$ to $100\mu m$, the diameters of the circular apertures range from $5''$ to $180''$ (Klaas et al., 1994). Aperture sequences on strong point sources behave differently from sequences on background positions (see Müller, 1999): The overall signal level is determined by the point source and the influence of the background is weak. Here the telescope-instrument point-spread-function (PSF) determines the signal for a given aperture (see Figure 1).

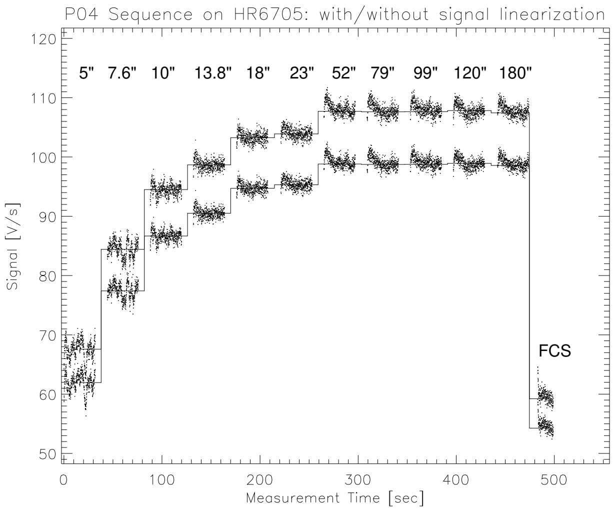

Figure 1. Effect of signal linearization on a bright point source (HR 6705 at 3.6 μm): Upper sequence with and lower sequence without signal linearization. The SRD data are given as dots, the SCP results in histogram mode. The total signal level is only changing by a few percent since the bright point source is always inside the apertures.

Observations of background positions are influenced by the peculiar, roof-shaped aperture profiles and the possible center to center offsets of the apertures. Extended sources and faint sources on a strong background are between these two extreme cases and have to be analysed carefully to distinguish between instrumental effects and real structures.

In the following section the measurements and the data reduction methods are described. The third section contains the calculation of the PSF and the discussion in combination with the aperture sequences. In Section 4. the method to determine the background contribution is presented, in Section 5. and Section 6. the theoretical considerations were combined with measurements, first for calibration sources and then for scientific targets. In the last section the results are discussed and conclusions, recommendations and an outlook are given. All results presented

*ISO is an ESA project with instruments funded by ESA Member States (especially the PI countries: France, Germany, the Netherlands and the United Kingdom) and with the participation of ISAS and NASA.

Table 2. Apertures photometry on the CAM CVF measurement of HD 97300.

Aper. Diam. [″]	Flux 7.5 μm [Jy]	r.m.s.	Flux 10.0 μm [Jy]	r.m.s.
6.0	1.07	0.01	0.27	0.01
12.0	2.30	0.01	0.67	0.01
18.0	3.73	0.02	1.23	0.02
24.0	4.68	0.02	1.64	0.02
30.0	5.49	0.03	2.00	0.03
36.0	6.01	0.04	2.22	0.03
42.0	6.46	0.04	2.39	0.04
48.0	6.93	0.05	2.57	0.04
54.0	7.28	0.05	2.72	0.05
60.0	7.46	0.06	2.81	0.05

here are based purely on sky measurements, neither internal calibration measurements nor aperture sequences on the FCS have been considered.

2. OBSERVATIONS AND DATAREDUCTION

All ISOPHOT calibration measurements on point sources, performed with the AOT PHT04 (Multi-aperture Photometry), are included in the following analysis with the exception of chopped and "corrupted" observations. One ISOCAM target has been analysed in detail to validate the PHT04 sequences. All observations are summarized in detail in Table 1.

2.1. ISOCAM DATA REDUCTION

The PHT aperture photometry of the Herbig Ae/Be star HD 97300 was compared with results of ISOCAM CVF (CAM04) measurements (Siebenmorgen et al., 1998). The measurements were taken with the 3" pixel scale and the small field mirror on September 24th, 1997. The basic data reduction steps are described in Siebenmorgen et al. (1997).

Close to the reference wavelength of the PHT measurements a multi-aperture photometry on the CVF images was simulated. The results are summarized in Table 2.

The apertures are centered on the brightest pixel, which corresponds to the nominal star position.

2.2. ISOPHOT DATA REDUCTION

All PHT-data have been processed with ISOPHOT Interactive Analysis (PIA[1]) V8.0 (Gabriel et al., 1997). Details about the data reduction and the discussion of the critical steps can be found in Paper I.

[1]PIA is a joint development by the ESA Astrophysics Division and the ISOPHOT consortium.

3. THEORETICAL CONSIDERATIONS

3.1. Monochromatic Modeling of a Point Source

In parallel to the measurements a Point Spread Function (PSF) model was developed to simulate aperture sequences on point and different types of extended sources (box-, gaussian, $1/\rho$-profile, ...). The monochromatic PSF-model includes the the $D = 60\,cm$ primary mirror with a central obscuration $\epsilon = 0.30$ by the secondary:

$$PSF(v) = \frac{1}{(1-\epsilon^2)^2}\left[\frac{2J_1(v)}{v} - \epsilon^2\frac{2J_1(\epsilon v)}{\epsilon v}\right]^2 \qquad (1)$$

$$v = \frac{\pi r}{\lambda f}$$

With J_1 being the first order Bessel function, r the radial distance in the focal plane in $[mm]$, λ the wavelength and $f = DF$ the focal length, with a focal ratio $F = 15$. The sizes of the apertures in $[mm^2]$ are given in Paper I.

3.2. Modeling of a Point Source in a Bandpass

A point source with a constant energy spectrum $\nu F_\nu = \lambda F_\lambda = const.$ was used in combination with the filter transmission $T(\lambda)$ curves to produce the Point Spread Function factors F_{psf} for a given band pass for all apertures.

$$F^a_{psf} = \frac{1}{N}\int\int\int PSF(\lambda, r, \phi)d\phi dr T(\lambda)F_\nu(\lambda)d\lambda \quad (2)$$

With N as the normalization factor. The wavelength integration $d\lambda$ goes over the full band pass, the radial integration dr from the center to the full aperture radius and $d\phi$ from 0 to 2π. The calculated values are given in Table 3. The values give the fraction of the total point source power seen by the detector pixel if centered on the pixel. The monochromatic F_{psf} values, as given in the ISOPHOT Observer's Manual (Klaas et al. 1994), deviate by up to 8 % from the values in Table 3.

3.3. Modeling of a Point Source on a Background

The background level strongly influences the aperture sequences. One can either treat the background influence by subtracting it from the measured signals or by including the background contribution in the theoretical modeling. Here the second approach has been followed to be able to include the results from Section 4. in a clean way. First the background contribution has been determined from the measurements in the following ways: Either a full aperture sequence on a background position exists which can be used directly in the modeling, or the background

Table 1. List of all Observations.

I. ISOCAM CVF observation

TDT	PROPID	DATE	AOT	FOV	Source	Observation
67901590	`RS_HEBE`	25-Sep-1997	CAM04	$96'' \times 96''$	HD 97300 Ring	CVF observation
67901591	`RS_HEBE`	25-Sep-1997	CAM01	$96'' \times 96''$	HD 97300 Ring off	general observation

II. ISOPHOT PHT04 on Point Sources

TDT	PROPID	DATE	AOT	Det/Fil	Apertures ["]	Source
05702505	`AOTPVP06`	13-Jan-96	P04	P1/3.6	5,7.6,10,13.8,18,23,52,79,99,120,180	HR 6705
05702506	`AOTPVP06`	13-Jan-96	P04	P1/12.0	10,13.8,18,23,52,79,99,120,180	HR 6705
87500104	`P04PSF02`	08-Apr-98	P04	P1/7.3	5,7.6,10,13.8,18,23,52,79,99,120,180	HR 7127
06101501	`AOTPVP6B`	17-Jan-96	P04	P2/25.0	23,52,79,99,120,180	HR 6705
72002402	`5412P204`	05-Nov-97	P04	P2/25.0	23,52,79,99,120,180	HR 7980
80500702	`P04PSF01`	18-Jan-98	P04	P2/25.0	23,52,79,99,120,180	HR 617
80500804	`P04PSF01`	18-Jan-98	P04	P2/20.0	10,13.8,18,23,52,79,99,120,180	HR 617
79600206	`P04PSF01`	19-Jan-98	P04	P3/60.0	10,13.8,18,23,52,79,99,120,180	HR 6705
80501508	`P04PSF01`	28-Jan-98	P04	P3/60.0	10,13.8,18,23,52,79,99,120,180	HR 337
81500710	`P04PSF01`	07-Feb-98	P04	P3/60.0	10,13.8,18,23,52,79,99,120,180	HR 1457

III. ISOPHOT PHT04 on HD 97300

TDT	PROPID	DATE	AOT	Det/Fil	Apertures ["]	Source
67901413	`APERTURE`	15-Sep-97	P04	P1/7.3	5,7.6,10,13.8,18,23,52,79,99,120,180	HD 97300
67901414	`APERTURE`	15-Sep-97	P04	P1/10.0	5,7.6,10,13.8,18,23,52,79,99,120,180	HD 97300

Table 3. Point spread function factors for all P-filters and apertures. The values are calculated for the bandpass, assuming a constant energy spectrum $\nu F_\nu = const.$ The influence of the energy spectrum on the F_{psf} values is minor, on the order of a few percent, depending on the spectral shape. λ_n is the nominal filter wavelength.

Filter	$\lambda_n[\mu m]$	$5''$	$7.5''$	$10''$	$13.8''$	$18''$	$23''$	$52''$	$79''$	$99''$	$120''$	$180''$
P_3.29	3.3	0.87	0.91	0.93	0.95	0.97	0.97	0.99	0.99	0.99	0.99	1.00
P_3.6	3.6	0.83	0.91	0.93	0.95	0.96	0.97	0.99	0.99	1.00	1.00	1.00
P_4.85	4.8	0.67	0.90	0.91	0.92	0.95	0.96	0.98	0.99	0.99	0.99	1.00
P_7.3	7.3	0.62	0.74	0.87	0.90	0.92	0.93	0.97	0.98	0.99	0.99	1.00
P_7.7	7.7	0.62	0.72	0.88	0.90	0.91	0.92	0.97	0.98	0.98	0.99	0.99
P_10	10.0	0.53	0.64	0.73	0.87	0.90	0.91	0.96	0.98	0.98	0.99	0.99
P_11.3	11.3	0.47	0.64	0.66	0.80	0.90	0.91	0.95	0.97	0.98	0.98	0.99
P_11.5	12.0	0.44	0.63	0.67	0.76	0.88	0.90	0.95	0.97	0.98	0.98	0.99
P_12.8	12.8	0.41	0.63	0.64	0.72	0.89	0.90	0.95	0.97	0.97	0.98	0.99
P_16.0	15.0	0.32	0.59	0.64	0.65	0.82	0.89	0.95	0.96	0.97	0.98	0.99
P_20	20.0	0.19	0.45	0.57	0.63	0.66	0.73	0.91	0.95	0.96	0.97	0.98
P_25	25.0	0.15	0.39	0.52	0.61	0.64	0.68	0.91	0.94	0.95	0.96	0.98
P_60	60.0	0.03	0.08	0.13	0.20	0.33	0.43	0.66	0.82	0.89	0.90	0.92
P_100	100.0	0.01	0.03	0.05	0.08	0.14	0.20	0.57	0.64	0.68	0.77	0.90

contribution has been determined from the 2 largest apertures. The results from calibration sequences on flat backgrounds (see Section 4.) and the pure PSF modeling (see Section 3.2.) have also been taken into account.

3.4. Modeling of Extended Sources

In order to be able to analyse the aperture sequences on extended sources, different sizes and profiles of point and extended emission have been tested out in combination with the theoretical PSF calculations. The following source profiles are included:

- flat distribution to model sequences on the background
- box function, with the box width equivalent to the source width
- gaussian function, with the FWHM as source width equivalent (see also Figure 2)
- $1/\rho$-distribution to model a comet coma brightness distribution

Additionally a background contribution can be added. This contribution was usually determined from the 2 largest apertures (see Section 4.).

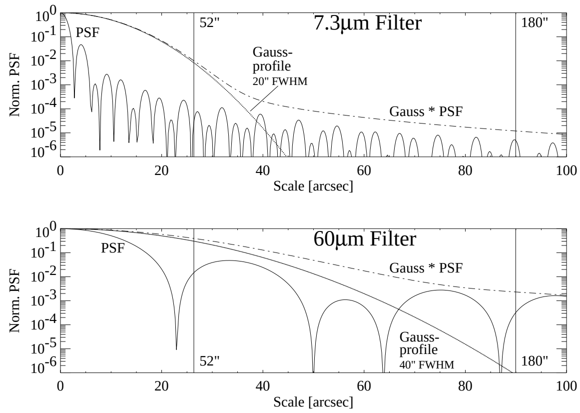

Figure 2. The modeled monochromatic PSF at 2 different wavelengths. The 52" and the 180" apertures are shown as solid vertical lines. Gauss profiles with 20" FWHM (upper plot) and 40" FWHM (lower plot) are shown as dotted lines, after convolution with the PSF as dotted-dashed lines.

3.5. Performing a Theoretical Aperture Sequence

The total theoretical flux within the given apertures has been calculated and normalized to the 180″ aperture. This artificial aperture sequence (with realistic values for the background taken from the real measurements) can now be compared with the processed signals from the scientific observations.

4. BACKGROUND DETERMINATION

4.1. From Off-source Sequences

Aperture sequences on bright background positions have been analysed in Paper I. The results show that the *background signal per aperture area* is not constant for all apertures. To give an example: at 7.3 μm the 52″ aperture sees approximately only 50% *signal per aperture area* as compared to the 180″ aperture. Table 3. from Paper I summarizes the results, which will be used in the following analysis.

4.2. From On-source Sequences

As a first step one can start with an aperture sequence on a point source and determine the background from the differences between the largest apertures, where the point source contribution is small. We are looking for the *background signal per aperture area* $\frac{bgr}{area}$ and the pure source signal *src*. The measured quantities are the signal in the 180″ aperture sig_{180} and the signal in the 120″ aperture sig_{120}. The contribution of the source in different apertures is given by the *point spread function factor* F_{psf} (see Table 3). The following assumptions were made:

$$\begin{aligned} sig_{aper} &= srcF_{psf}^{aper} + \frac{bgr}{area} area_{180} \times \delta_{aper} \quad (3) \\ total &= source + background \times correction \end{aligned}$$

The background correction $\delta_{aperture}$ can be neglected when calculating the total source signal from the 180" or the 120" aperture. Therefore the source signal is the following:

$$src = \frac{sig_{aper} - \frac{bgr}{area} area_{aper}}{F_{psf}^{aper}} \quad (4)$$

Which allows to determine the $\frac{bgr}{area}$ value from the signals in the 180" and the 120" aperture:

$$\frac{bgr}{area} = \frac{sig_{180} - sig_{120} F_{psf}^{180}/F_{psf}^{120}}{area_{180} - area_{120} F_{psf}^{180}/F_{psf}^{120}} \quad (5)$$

Now the background contribution can be calculated for different apertures, taking also the corrections from Paper I into account. Example: The background in the 180″ aperture is $\frac{bgr}{area} area_{180} \times 1.0$ and in the 52″ aperture $\frac{bgr}{area} area_{52} \times 0.5$ at $7.3\,\mu m$. And so on for the other apertures.

This method to determine the background from the on-source sequence has the advantage that the detector "sees" at the same time the source and the background, therefore the orbit-dependent responsivity is not relevant (assuming that the responsivity does not change during one measurement sequence). If we want to take the off-source aperture sequence we first have to find a way to calibrate both sequences on an absolute scale, a simple signal subtraction does usually not work. Another advantage of this background determination method is the relatively stable signal level, since the source which determines to a large fraction the total signal level, is always within the beam. While the pure background sequences suffer from a hugh signal change from small to large apertures. A clear disadvantage of this method is that the fraction of the scientific source falling into different apertures is a priori not known. But here one can solve the problem iteratively by modeling an extended source, calculating the F_{psf} values and comparing with the measured signals. The source extension and also the source brightness profile have to be changed iteratively until the model and the measurement agrees.

5. SEQUENCES ON POINT SOURCES

With Equation 4 one can determine the total signal only produced by the source and with Equation 5 the signal fraction of the background in each aperture. Adding up both, source and background signal, for each aperture one can predict the signal behaviour for all apertures. Therefore the theoretical PSF modeling in combination with the signal information from the 2 largest apertures are now sufficient to analyse PHT04 sequences on point sources. Figures 3, 4 and 5 show the comparison between model and measurement.

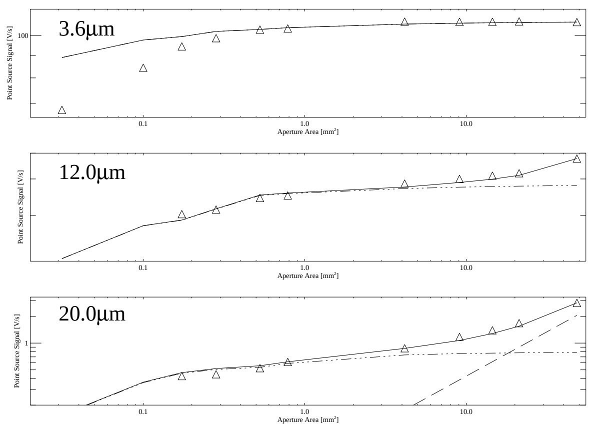

Figure 3. Aperture sequence on a point source. The solid line is the prediction from the model PSF, including the background contribution as measured from the 2 largest apertures. The dashed lines indicate the pure source and background contribution for all apertures.

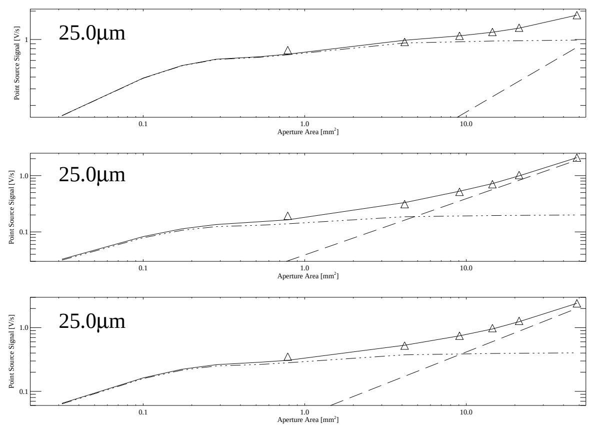

Figure 4. Caption see Figure 3. The sources are HR 6705, HR 7980 and HR 617 (from upper to lower plot).

The measured PSF values agree quite well with the theoretical predictions. Only for the small apertures at 3.6 μm and at 60.0 μm there are deviations. These offsets could be explained by slight off-center positions of the small apertures relative to the larger ones and by the simplified PSF model, which does not take the tripod of the secondary telescope mirror into account. In the plot the pure source (dotted-dashed line) and the pure background (dashed line) contribution are also plotted.

For the smallest apertures at short wavelengths the pointing jitter of the telescope influences also measurements. In Figure 1 the signal variations in the smallest apertures are caused by the telescope pointing jitter. The source is moving within the aperture, with the intensity peak close to the edge of the aperture, and the signal changes accordingly. The derived source signals (solid lines) are therefore underestimated. This is also reflected in Figure 3

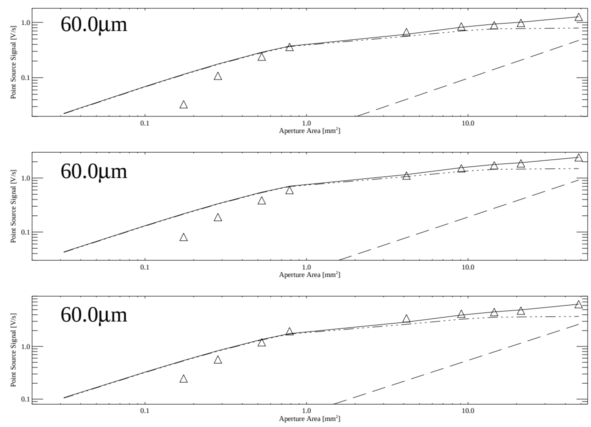

Figure 5. Caption see Figure 3. The sources are HR 6705, HR 337 and HR 1457 (from upper to lower plot).

6. SEQUENCES ON SCIENCE TARGETS

The aperture sequences on HD 97300 have been investigated in the same way as described above: the two largest apertures have been used to derive the pure *source*-signal and the *background signal per aperture area*. With these results the model has been started, first only for a pure point source (see upper part of Figure 6 and Figure 7, where the model fails to explain the measured signals) and then for an extended source (lower part).

The extended source was modeled assuming a Gaussian brightness distribution with a FWHM of 28 $arcsec$ (7.3 μm) and 35 $arcsec$ (10.0 μm). From the ISOCAM images Siebenmorgen *et al.* (1998) derived an extension for the ring of organic molecules around HD 97300 of approximately $50 \times 36\,arcsec$. Taking our simplified gaussian distribution of the brightness into account, the derived FWHM from PHT04 sequences and the CAM exposures agree quite well. The fact that in the CAM CVF lw5 (centered at 6.8 μm) the continuum emission dominates and in the lw8 (centered at 11.3 μm) a central point source is visible in the frames is also reflected in the aperture sequences: At 10.0 μm the measured signal in the smallest aperture stays constant which is caused by the point source in the center. At 10.0 μm the gaussian distribution fits almost perfectly the measured signals. Only the innermost aperture deviates slightly.

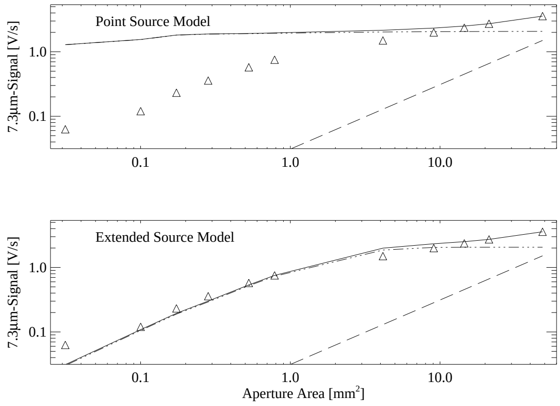

Figure 6. PHT04 Observations (triangles) and modeling of HD 97300 at 7.3 μm. The point source model is given in the upper panel, the extended source model (FWHM of 28 arcsec) in the lower panel. The pure source contribution is shown in dotted-dashed lines, the pure background in dashed lines.

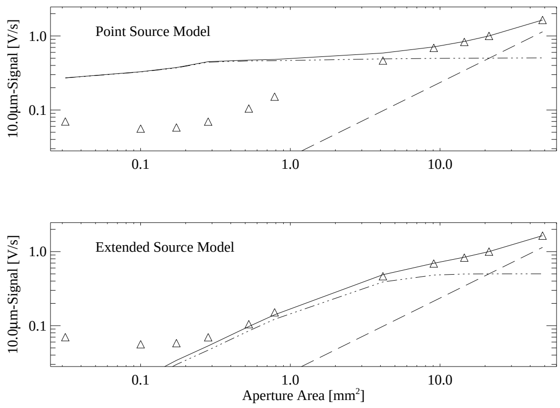

Figure 7. PHT04 Observations (triangles) and modeling of HD 97300 at 10.0 μm. The point source model is given in the upper panel, the extended source model (FWHM of 35 arcsec) in the lower panel. The pure source contribution is shown in dotted-dashed lines, the pure background in dashed lines.

7. CONCLUSIONS

With the knowledge of the aperture profiles and the assumption that some apertures are slightly off-center one can understand the ISOPHOT aperture sequences to a large extend. With the additional corrections of the signal linearization it was for the first time possible to analyse the PHT04 observations in a consistent way without using the internal calibration source (FCS), which is not yet calibrated in "non-standard" apertures. With the results presented here it is not only possible to distinguish clearly between point- and extended sources but also to determine the extension of a source on *arcsec* scale.

Acknowledgements

Part of this work was done at the Max-Planck-Institut für Astronomie (MPIA) in Heidelberg. I thank Carlos Gabriel, Ulrich Klaas, Rene Laureijs and Bernhard Schulz for many discussions and comments on the paper. I thank Ralf Siebenmorgen for providing the aperture photometry of HD 97300 from CAM CVF measurements. I also would like to thank Bernhard Schulz for presenting these results at the workshop "ISO beyond point sources: Studies of extended infrared emission".

REFERENCES

Gabriel, C., Schulz, B., Acosta–Pulido, J. A. *et al.* 1997, Proc. of ADASS VI, 112

Heinrichsen, I., Dec 1997, ISOPHOT Internal Report: "Report on First Results of P04 Multi-aperture Photometry Calibration Programme Pilot Observation"

Kessler M.F., Steinz J.A., Anderegg M.E., *et al.* 1996 A&A 315, L27

Klaas, U., Krüger, H.Heinrichsen, I. *et al.* 1994, ISOPHOT Observer's Manual, ESA/ESTEC, Noordwijk, Version 3.1

Klaas, U., Laureijs, R.J., Radovich, M. and Schulz, B. 1998, Calibration Accuracies (http://www.iso.vilspa.esa.es/manuals/PHT/accuracies/pht_accuracies20/)

Laureijs R.J., Klaas U., Richards PlJ. *et al.* 1998, ISOPHOT Data Users Manual, SAI/95-220/Dc, Version 4.0, Appendix C: Colour Corrections

Lemke D., Klaas U., Abolins J., *et al.* 1996, A&A 315, L64

Müller, T.G., 1999, same proceedings, "ISOPHOT APERTURE PROFILES AND BACKGROUND MEASUREMENTS"

Siebenmorgen, R., Natta, A., Krügel, E., Prusti, T., 1998, A&A 339, 134

Siebenmorgen, R., Starck, J.L., Cesarsky D.A., *et al.* 1997, ESA document SAI/95-222/Dc